Syntheses, Crystal Structures and Electrochemical Properties of Acetylacetonato-Ruthenium Complexes Containing Substituted Pyridine Ligands

Xiuli Wu[a], Rufei Ye[a,b], Ai-Quan Jia[b], Qun Chen[a], and Qian-Feng Zhang[a,b]

[a] Department of Applied Chemistry, School of Petrochemical Engineering, Changzhou University, Jiangsu 213164, P. R. China

[b] Institute of Molecular Engineering and Applied Chemistry, Anhui University of Technology, Ma'anshan, Anhui 243002, P. R. China

Reprint requests to Dr. Qian-Feng Zhang. Fax: +86-555-2312041. E-mail: zhangqf@ahut.edu.cn

Z. Naturforsch. **2013**, *68b*, 993 – 999 / DOI: 10.5560/ZNB.2013-2344
Received December 31, 2012

Treatment of $Ru(acac)_3$ with 2-cyano-pyridine and 3,5-dimethyl-pyridine in the presence of zinc dust as reducing agent in refluxing THF afforded the ruthenium(II) complexes *cis*-$[Ru^{II}(acac)_2(2\text{-}CN\text{-}py)_2]$ (**1**) and *cis*-$[Ru^{II}(acac)_2(3,5\text{-}Me_2\text{-}py)_2]$ (**2**), respectively. Interaction of $Ru(acac)_3$ with 3-Me-pyridine and 3,5-Me_2-pyridine in the presence of Br_2 in refluxing THF gave the ruthenium(III) complexes $[Ru^{III}(acac)Br_2(3\text{-}Me\text{-}py)_2]$ (**3**) and $[Ru^{III}(acac)Br_2(3,5\text{-}Me_2\text{-}py)_2]$ (**4**), respectively. The four complexes have been spectroscopically and electrochemically characterized, and their crystal and molecular structures have been established by X-ray crystallography.

Key words: Ruthenium, Acetylacetonato Ligand, Pyridine, Synthesis, Crystal Structure

Introduction

Tris(acetylacetonato)ruthenium(III), $Ru(acac)_3$, belongs to a wide series of typical $M(acac)_3$ complexes which have been intensively studied by physical techniques since they are representative in their properties of many complexes [1]. Recently, single-crystal X-ray structure determinations at room and lower temperatures for $Ru(acac)_3$, together with powder neutron diffraction experiments, have provided auxiliary data allowing magnetic structures/factors to be deduced from the polarized neutron diffraction experiments [2]. From the view point of synthetic chemistry, $Ru(acac)_3$ has proven to be a versatile precursor for a variety of organometallic complexes [3−6]. For example, catalytic hydrogen reduction of $Ru(acac)_3$ gave the diacetonitrile-bis(β-diketonato)ruthenium(II) complex $[Ru^{II}(acac)_2(CH_3CN)_2]$ [7]; the acetonitrile ligands of the resulting species could be substituted by more electron-donating ligands, *e. g.*, phosphines [8, 9], pyridine [10−12], *o*-aminoquinone [13], and β-ketiminates [14]. The reaction of $Ru(acac)_3$ with an excess of diene in the presence of zinc as reducing agent afforded a series of pseudo-octahedral $Ru(acac)_2$(diene) complexes [6]. The reflux of $[Ru^{II}(acac)_2(CH_3CN)_2]$ in 2-methyl-2-propanol gave the novel diamagnetic tetranuclear β-diketonato ruthenium complex $[Ru(\mu\text{-}acac)_2(\mu_3\text{-}O)_2Ru_3(acac)_6]$ [15]. Alcoholic solutions of $Ru(acac)_3$ were saturated by bubbling CO under radiolysis, leading to the isolation of the ruthenium(II) carbonyl complexes $[Ru(acac)_2(CO)L]$ (L = MeOH, EtOH or *i*-PrOH) in which the alcohol molecules are readily displaced by stronger donors [16]. It is prospected that compounds $[Ru(acac)_2(CO)L]$ may be good precursors for a wide range of ruthenium(II) complexes containing oxygen, nitrogen or sulfur donor ligands. To further understand the ligand effect of $Ru(acac)_3$ owing to the delocalization of negative charge over five atoms in $acac^-$, we were interested to investigate the reactivity of $Ru(acac)_3$ with pyridine under reducing or oxidizing conditions, which results in the formation of $[Ru^{II}(acac)_2]$ and $[Ru^{III}(acac)]$ species with substituted pyridine ligands. The results including the structural

characterization and electrochemical properties of the ruthenium-acac-pyridine complexes are presented in this paper.

Experimental

General

All synthetic manipulations were carried out under dry nitrogen by standard Schlenk techniques. $Ru(acac)_3$ was prepared according to the literature [17]. $RuCl_3 \cdot 3H_2O$ was used as purchased from Pressure Chemical Co. Ltd. NMR spectra were recorded on a Bruker ALX 300 spectrometer operating at 300 MHz for ^1H, and chemical shifts δ (in ppm) were reported with reference to $SiMe_4$ (^1H). Infrared spectra were recorded on a Perkin-Elmer 16 PC FT-IR spectrophotometer with use of KBr pellets, and positive FAB mass spectra were recorded on a Finnigan TSQ 7000 spectrometer. The magnetic moment of the solid samples was measured by a Sherwood magnetic susceptibility balance at room temperature. Cyclic voltammetry was performed on a CHI 660 electrochemical analyzer. A standard three-electrode cell was used with a glassy carbon working electrode, a platinum counterelectrode and an Ag/AgCl reference electrode under nitrogen atmosphere at 25 °C. Formal potentials (E^o) were measured in CH_2Cl_2 solutions with 0.1 M $[n\text{-}Bu_4N]PF_6$ as supporting electrolyte and reported with reference to the ferrocenium-ferrocene couple ($Cp_2Fe^{+/0}$). In the −2.0 to +1.5 V region, a potential scan rate of 50 mV s^{-1} was used. Elemental analyses were carried out using a Perkin-Elmer 2400 CHN analyzer.

*Synthesis of cis-[Ru^{II}(acac)$_2$(2-CN-py)$_2$]·$^1/_4H_2O$ (**1**·$^1/_4H_2O$)*

To a THF (10 mL) solution of $Ru(acac)_3$ (80 mg, 0.2 mmol) were added 2-CN-py (124 mg, 1.2 mmol) and zinc dust (1.0 g) under nitrogen. The reaction mixture was refluxed for 4 h, developing a bright-red color. The solvent was removed *in vacuo*, and the residue was extracted with CH_2Cl_2 (3 × 5 mL) and filtered through a coarse funnel frit padded with celite. The resulting red solution was concentrated to *ca.* 1 mL. Column chromatography of the red concentrated solution on silica gel using CH_2Cl_2-hexane (1 : 9, *v*/*v*) as eluant gave a bright-red band, which was eluted and evaporated to dryness. The sticky residue was washed with diethyl ether to give pure *cis*-[Ru^{II}(acac)$_2$(2-CN-py)$_2$] (**1**) as a red solid. Yield: 49 mg, 48% (based on Ru). Single crystals of **1**·$^1/_4H_2O$ were obtained by recrystallization from CH_2Cl_2-hexane containing traces of water within three days. $-^1H$ NMR (300 MHz, $CDCl_3$): $\delta = 1.51$ (br, H_2O), 1.71 (s, 3H, CH_3(acac)), 1.76 (s, 3H, CH_3(acac)), 1.93 (s, 3H, CH_3(acac)), 2.02 (s, 3H, CH_3(acac)), 4.83 (s, 1H, CH(acac)), 4.97 (s, 1H, CH(acac)), 7.76 (dd, $J = 6.8$ Hz, 2H, py), 7.89 (dd, $J = 6.4$ Hz, 2H, py), 8.13 (dd, $J = 6.7$ Hz, 2H, py), 8.21 (dd, $J = 6.3$ Hz, 2H, py) ppm. – IR (KBr disc, cm^{-1}): ν(C≡N) 2163 (vs), ν(C=N) 1591 (s), ν(C=O) 1422 (s), ν(C−O) 1086 (s) and 1025 (s). – MS (FAB): $m/z = 507$ $[M]^+$, 309 $[Ru(2\text{-}CN\text{-}py)_2]^+$, 299 $[Ru(acac)_2]^+$. – Anal. for $C_{22}H_{22}N_4O_4Ru \cdot {}^1/_4H_2O$: calcd. C 51.61, H 4.23, N 10.94; found C 51.42, H 4.21, N 10.78.

*Synthesis of cis-[Ru^{II}(acac)$_2$(3,5-Me$_2$-py)$_2$] (**2**)*

The method was similar to that used for complex **1**, employing 3,5-Me_2-py (128 mg, 1.2 mmol) instead of 2-CN-py. Yield: 51 mg, 50% (based on Ru). Single crystals of **2**·$^1/_3$NaBr·4.5H_2O were obtained by recrystallization from MeOH-Et_2O in the presence of aqueous sodium bromide within two days. Its composition resulted from the refined crystal structure (see below). $-^1H$ NMR (300 MHz, $CDCl_3$): $\delta = 1.29$ (s, 6H, CH_3py), 1.32 (s, 6H, CH_3py), 1.55 (br, H_2O), 1.75 (s, 3H, CH_3(acac)), 1.79 (s, 3H, CH_3(acac)), 1.92 (s, 3H, CH_3(acac)), 2.7 (s, 3H, CH_3(acac)), 4.92 (s, 1H, CH(acac)), 5.06 (s, 1H, CH(acac)), 7.81 (dd, $J = 7.1$ Hz, 2H, py), 7.94 (dd, $J = 7.2$ Hz, 2H, py), 8.11 (dd, $J = 6.9$ Hz, 2H, py), 8.21 (dd, $J = 6.3$ Hz, 2H, py) ppm. – IR (KBr disc, cm^{-1}): ν(C=N) 1597 (s), ν(C=O) 1436 (s), ν(C−O) 1091 (s) and 1037 (s). – MS (FAB): $m/z = 505$ $[M]^+$, 307 $[Ru(3,5\text{-}Me_2\text{-}py)_2]^+$, 299 $[Ru(acac)_2]^+$. – Anal. for $C_{24}H_{32}N_2O_4Ru \cdot {}^1/_3NaBr \cdot 4.5H_2O$: calcd. C 45.86, H 6.57, N 4.46; found C 46.42, H 6.33, N 4.48.

*Synthesis of [Ru^{III}(acac)Br$_2$(3-Me-py)$_2$] (**3**)*

To a THF (10 mL) solution of $Ru(acac)_3$ (80 mg, 0.2 mmol) were added 3-Me-py (112 mg, 1.2 mmol) and Br_2 (0.35 g) under nitrogen. The reaction mixture was refluxed for 8 h, developing a dark-red color. The solvent was evaporated *in vacuo*, and the residue was washed with hexane (2 × 5 mL). Recrystallization from CH_2Cl_2-hexane afforded red crystals of **3** within a week. Yield: 73 mg, 67% (based on Ru). – IR (KBr disc, cm^{-1}): ν(C=N) 1583 (s), ν(C=O) 1427 (s), ν(C−O) 1096 (s) and 1032 (s). – MS (FAB): $m/z = 786$ $[M]^+$, 707 $[M\text{–}Br]^+$, 628 $[M\text{–}Br]^+$, 307 $[Ru(3\text{-}Me\text{-}py)_2]^+$, 200 $[Ru(acac)]^+$. – $\mu_{eff} = 1.97$ μ_B. – Anal. for $C_{17}H_{21}N_2O_2Br_5Ru$: calcd. C 25.98, H 2.69, N 3.56; found C 25.84, H 2.63, N 3.51.

*Synthesis of [Ru^{III}(acac)Br$_2$(3,5-Me$_2$-py)$_2$] (**4**)*

The method was similar to that used for complex **3**, employing 3,5-Me_2-py (128 mg, 1.2 mmol) instead of 3-Me-py. Yield: 52 mg, 45% (based on Ru). – IR (KBr disc, cm^{-1}): ν(C=N) 1581 (s), ν(C=O) 1424 (s), ν(C−O) 1089 (s) and 1023 (s). – MS (FAB): $m/z = 574$ $[M]^+$, 495 $[M\text{−}Br]^+$, 416 $[M\text{−}Br]^+$, 287 $[Ru(3\text{-}Me\text{-}py)_2]^+$, 200 $[Ru(acac)]^+$. – $\mu_{eff} = 1.93$ μ_B. – Anal. for $C_{19}H_{25}N_2O_2Br_2Ru$: calcd. C 39.74, H 4.39, N 4.88; found C 39.82, H 4.35, N 4.81.

Table 1. Crystallographic data and numbers pertinent to data collection and structure refinement for *cis*-[Ru^{II}(acac)$_2$(2-CN-py)$_2$]·$^1/_4H_2O$ (**1**·$^1/_4H_2O$), *cis*-[Ru^{II}(acac)$_2$(3,5-Me_2-py)$_2$]·$^1/_3$NaBr·4.5H_2O (**2**·$^1/_3$NaBr·4.5H_2O), [Ru^{III}(acac)Br_2(3-Me-py)$_2$] (**3**), and [Ru^{III}(acac)Br_2(3,5-Me_2-py)$_2$] (**4**).

Compound	**1**·$^1/_4H_2O$	**2**·$^1/_3$NaBr·4.5H_2O	**3**	**4**
Empirical formula	$C_{22}H_{22.5}N_4O_{4.25}Ru$	$C_{24}H_{41}N_2O_{8.5}Ru{\cdot}Na_{0.33}Br_{0.33}$	$C_{17}H_{21}N_2O_2Br_5Ru$	$C_{19}H_{25}N_2O_2Br_2Ru$
Formula weight	512.01	617.7	546.25	574.30
Crystal system	monoclinic	trigonal	monoclinic	monoclinic
Space group	$C2/c$	$R\bar{3}c$	$P2_1/c$	$C2/c$
a, Å	35.230(11)	22.749(4)	14.789(8)	30.85(3)
b, Å	8.465(3)	22.749(4)	9.114(5)	9.131(8)
c, Å	16.806(5)	30.05(1)	15.404(8)	15.718(3)
β, deg	115.172(5)		109.085(10)	94.12(2)
V, Å^3	4536(2)	13468(5)	1962.1(18)	4417(7)
Z	8	18	4	8
$D_{calcd.}$, g cm^{-3}	1.50	1.40	1.85	1.73
Temperature, K	296(2)	296(2)	296(2)	296(2)
F(000), e	2084	5886	1068	2264
μ(Mo$K\alpha$), mm^{-1}	0.7	1.0	4.9	4.3
Total refls.	11449	27271	12044	13859
Independent refls. / R_{int}	4890 / 0.0228	3370 / 0.0681	4422 / 0.0489	5057 / 0.0672
Ref. parameters	294	185	221	241
$R1$[a] / $wR2$[b] [$I > 2\,\sigma(I)$]	0.0274 / 0.645	0.0464 / 0.0789	0.0519 / 0.1072	0.0491 / 0.1002
$R1$ / $wR2$ (all data)	0.0381 / 0.695	0.0663 / 0.1278	0.0677 / 0.1213	0.1065 / 0.1223
Goodness of fit (GoF)[c]	1.5	1.1	1.2	0.97
Final max / min difference peaks, e Å^{-3}	+00.39 / −0.26	+0.73 / −0.39	+10.40 / −1.63	+0.71 / −0.82

[a] $R1 = \Sigma||F_o| - |F_c||/\Sigma|F_o|$; [b] $wR2 = [\Sigma w(F_o^2 - F_c^2)^2/\Sigma w(F_o^2)^2]^{1/2}$, $w = [\sigma^2(F_o^2) + (AP)^2 + BP]^{-1}$, where $P = (\mathrm{Max}(F_o^2, 0) + 2F_c^2)/3$; [c] GoF $= [\Sigma w(F_o^2 - F_c^2)^2/(n_{obs} - n_{param})]^{1/2}$.

X-Ray crystallography

Crystallographic data and experimental details for *cis*-[Ru^{II}(acac)$_2$(2-CN-py)$_2$]·$^1/_4H_2O$ (**1**·$^1/_4H_2O$), *cis*-[Ru^{II}(acac)$_2$(3,5-Me_2-py)$_2$]·$^1/_3$NaBr·4.5H_2O (**2**·$^1/_3$NaBr·4.5H_2O), [Ru^{III}(acac)Br_2(3-Me-py)$_2$] (**3**), and [Ru^{III}(acac)Br_2(3,5-Me_2-py)$_2$] (**4**) are summarized in Table 1. Intensity data were collected on a Bruker SMART APEX 2000 CCD diffractometer using graphite-monochromatized MoK_α radiation ($\lambda = 0.71073$ Å) at 296(2) K. The collected frames were processed with the software SAINT [18]. The data were corrected for absorption using the program SADABS [19]. The structures were solved by Direct Methods and refined by full-matrix least-squares on F^2 using the SHELXTL software package [2, 21]. All non-hydrogen atoms were refined anisotropically. The positions of all hydrogen atoms were generated geometrically (C_{sp^3}–H = 0.97 and C_{sp^2}–H = 0.93 Å), assigned isotropic displacement parameters, and allowed to ride on their respective parent carbon or nitrogen atoms before the final cycle of least-squares refinement. The interstitial water molecules in **2**·$^1/_3$NaBr·4.5H_2O were anistropically refined without hydrogen atoms.

CCDC 917003–917006 contain the supplementary crystallographic data for this paper. These data can be obtained free of charge from The Cambridge Crystallographic Data Centre *via* www.ccdc.cam.ac.uk/data_request/cif.

Results and Discussion

The reaction of Ru(acac)$_3$ with an excess of the substituted pyridines and zinc as reducing agent in refluxing THF followed by chromatographic work-up of the initial product using a silica gel column resulted in the diamagnetic ruthenium(II) complexes *cis*-[Ru^{II}(acac)$_2$(2-CN-py)$_2$] (**1**) and *cis*-[Ru^{II}(acac)$_2$(3,5-Me_2-py)$_2$] (**2**). One acac$^-$ ligand in the starting complex dissociated from the ruthenium atom, and two pyridine ligands coordinated to the ruthenium center, six-coordinated *cis*-complexes being formed. Although the solids of both complexes are air-stable for months, partial air oxidation of the solutions occurs over a period of hours and results in shifting and broadening of the NMR peaks due to the presence of paramagnetic ruthenium(III) species. Treatment of Ru(acac)$_3$ with an excess of the substituted pyridines in the presence of Br_2 in refluxing THF afforded the neutral paramagnetic ruthenium(III) complexes [Ru^{III}(acac)Br_2(3-Me-py)$_2$] (**3**) and [Ru^{III}(acac)Br_2(3,5-Me_2-py)$_2$] (**4**) as dark-red solids, as illustrated in Scheme 1. Both complexes are formed by displacement of two acac$^-$ ligands in the ruthenium starting material by two pyri-

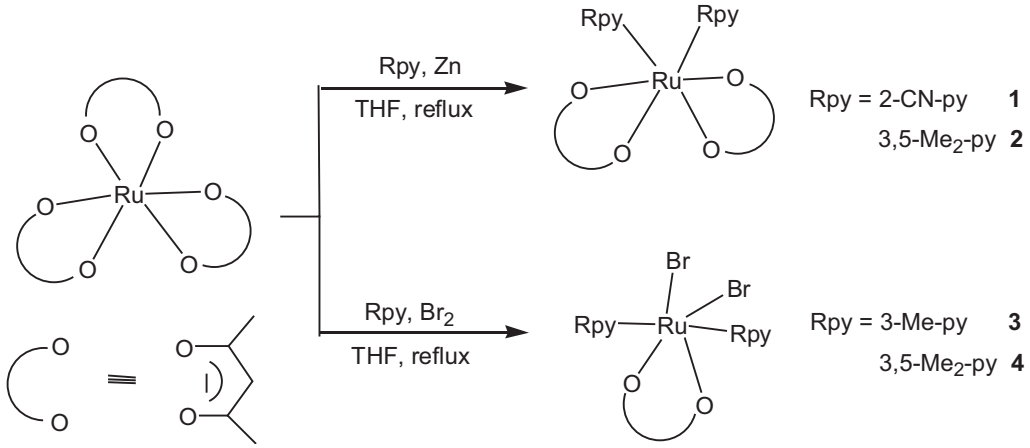

Scheme 1.

dine molecules and two bromide anions. No oxidation and reduction occurs in this reaction. Complexes **3** and **4** are of high solubility in most organic solvents and air-stable in both solid state and solution.

The IR spectrum of **1** clearly shows a strong band at 2163 cm^{-1} which may be attributed to the ν(C≡N) absorption. The bands at 1020−1440 cm^{-1} for ν(C=O) and ν(C−O) in the IR spectra indicate the presence of acac in all four complexes, complemented by a strong band at 1580−1600 cm^{-1} indicative of the ligand pyridine. The effective magnetic moments μ_{eff} of 1.97 and 1.93 μ_B at room temperature are consistent with the ruthenium(III) formulation for **3** and **4**, respectively. The two complexes are paramagnetic with one unpaired electron, consistent with the trivalent state of ruthenium (low-spin d^5, $S = {}^1/_2$) [22]. The ^{1}H NMR spectra of **1** and **2** show four signals at 1.3−2.1 ppm and two signals at 4.8−5.1 ppm corresponding to the methyl groups and the methyne protons of the acac ligands, respectively, indicating that the two substituted pyridines are *cis* to each other which makes the Me groups of acac inequivalent. The positive ion FAB mass spectra of the four complexes display the expected peaks which correspond to the molecular ions $[M]^+$, and to $[Ru(Rpy)_2]^+$ and $[Ru(acac)_2]^+$ / $[Ru(acac)]^+$ with the characteristic isotopic distribution patterns.

The molecular geometries of *cis*-[Ru^{II}(acac)$_2$(2-CN-py)$_2$] (**1**), *cis*-[Ru^{II}(acac)$_2$(3,5-Me_2-py)$_2$] (**2**), [Ru^{III}(acac)Br_2(3-Me-py)$_2$] (**3**), and [Ru^{III}(acac)Br_2(3,5-Me_2-py)$_2$] (**4**) are shown in Figs. 1–4, together with their atom numbering. Single crystals of **2** were obtained in the form of **2**·${}^1/_3$NaBr·4.5H_2O by recrystallization from MeOH-Et_2O in the presence of aqueous sodium bromide. Repeated cyrstallization attempts without

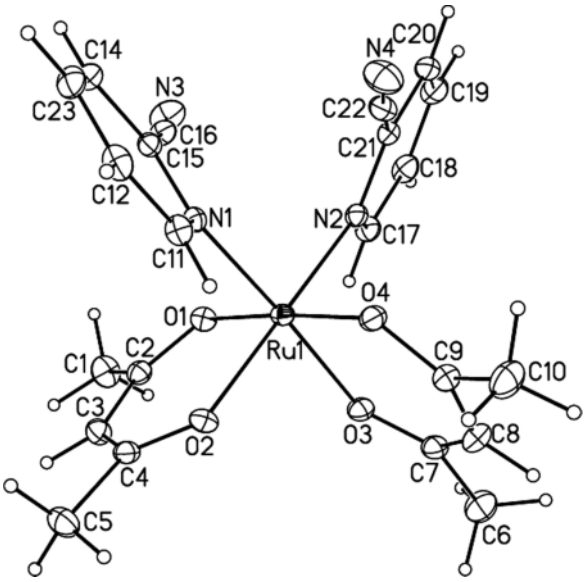

Fig. 1. Molecular structure of *cis*-[Ru^{II}(acac)$_2$(2-CN-py)$_2$] (**1**). The ellipsoids are drawn at the 35% probability level. Selected bond lengths (Å) and angles (deg): Ru(1)–O(1) 2.0412(17), Ru(1)–O(2) 2.0446(17), Ru(1)–O(3) 2.0459(16), Ru(1)–O(4) 2.0491(17), Ru(1)–N(1) 2.0328(18), Ru(1)–N(2) 2.0436(19); O(1)–Ru(1)–O(2) 92.57(7), O(3)–Ru(1)–O(4) 92.42(7), N(1)–Ru(1)–N(2) 94.68(7).

the presence of aqueous sodium bromide failed, however.

In all cases, the ligand environment about the ruthenium center is close to octahedral, and the configurations and compositions agree with those deduced on the basis of spectroscopic and microanalytical data. The bond lengths for Ru(III)−N(py) (av. 2.098(4) Å for **3** and av. 2.091(4) Å for **4**) are slightly longer than those for Ru(II)−N(py) (av. 2.038(2) Å for **1** and av. 2.081(4) Å for **2**). The Ru−O(acac) bond lengths of complexes **1**−**4** are generally in the range 2.01−2.09 Å, and thus similar to those in other $Ru^{II}(acac)_2$- and $Ru^{III}(acac)_2$-containing complexes [5−14]. The *cis* angles involving the two pyridine ligands, N(py)−Ru−N(py), are 92.57(7) and 92.45(19)° in **1** and **2**, respectively, while the *trans* angles N(py)−Ru−N(py) are 173.24(16) and 173.70(17)° in **3** and **4**, respectively. The average *cis* angles between the interchelate donor centers, O(acac)−Ru−O(acac), are 92.50(7)° in **1** and 91.98(14)° in **2**, and thus more obtuse than those of 90.58(15)° in **3** and 90.39(17)° in **4**. The average Ru−Br bond lengths of 2.470(1) Å in **3** and 2.487(2) Å in **4** are significantly shorter than that of 2.5524(4) Å in *trans*-[$(RuBr(py)_2(\mu$-pz)$]_2[PF_6]_2$ (pz = pyrazine) owing to the strong σ-donor capacity of the pyridine ligands [23]. The av-

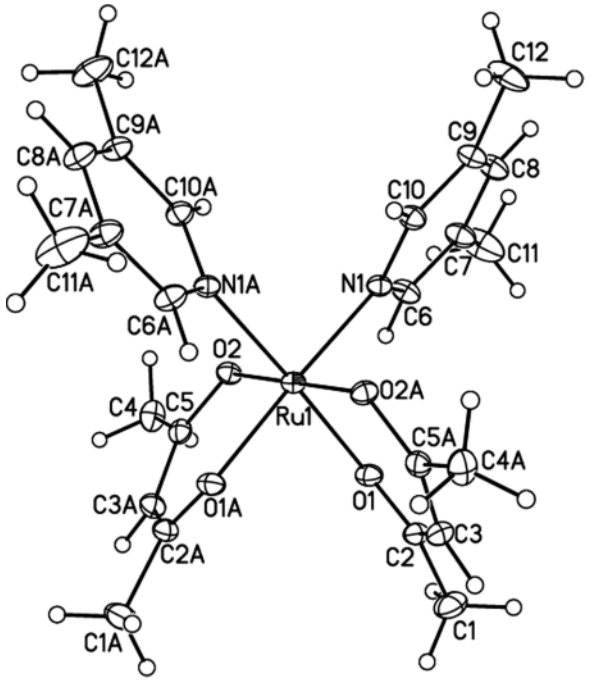

Fig. 2. Molecular structure of *cis*-$[Ru^{II}(acac)_2(3,5\text{-}Me_2\text{-}py)_2]$ (**2**) (ellipsoids at the 35% probability level). Selected bond lengths (Å) and angles (deg): Ru(1)–O(1) 2.020(3), Ru(1)–O(2) 2.007(3), Ru(1)–N(1) 2.081(4); O(2)#1–Ru(1)–O(1) 91.98(14), O(2)–Ru(1)–O(1)#1 91.99(14), N(1)#1–Ru(1)–N(1) 92.45(19) (#1 $y+{}^1/_3, x-{}^1/_3, -z+{}^1/_6$).

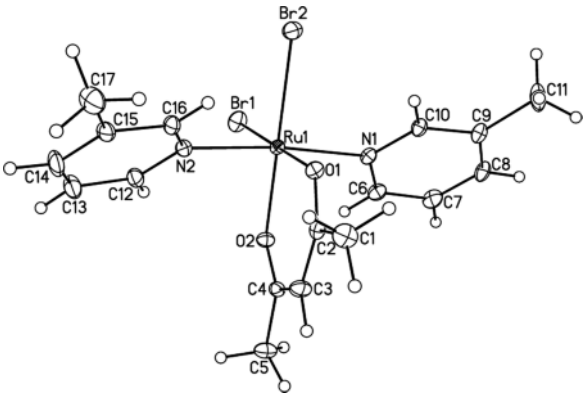

Fig. 3. Molecular structure of $[Ru^{III}(acac)Br_2(3\text{-Me-py})_2]$ (**3**) (ellipsoids at the 35% probability level). Selected bond lengths (Å) and angles (deg): Ru(1)–O(1) 2.010(3), Ru(1)–O(2) 2.023(3), Ru(1)–N(1) 2.103(4), Ru(1)–N(2) 2.093(5), Ru(1)–Br(1) 2.4704(11), Ru(1)–Br(2) 2.4698(12); O(1)–Ru(1)–O(2) 90.58(15), N(2)–Ru(1)–N(1) 173.24(16), Br(2)–Ru(1)–Br(1) 91.86(5), N(2)–Ru(1)–Br(2) 91.46(12), N(1)–Ru(1)–Br(2) 93.28(12), N(2)–Ru(1)–Br(1) 93.06(12), N(1)–Ru(1)–Br(1) 91.60(11).

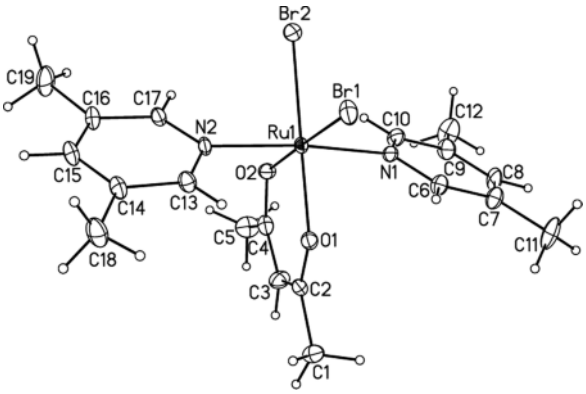

Fig. 4. Molecular structure of $[Ru^{III}(acac)Br_2(3,5\text{-}Me_2\text{-py})_2]$ (**4**) (ellipsoids at the 35% probability level). Selected bond lengths (Å) and angles (deg): Ru(1)–O(1) 2.028(4), Ru(1)–O(2) 2.011(4), Ru(1)–N(1) 2.089(4), Ru(1)–N(2) 2.093(4), Ru(1)–Br(1) 2.4706(17), Ru(1)–Br(2) 2.5025(18); O(2)–Ru(1)–O(1) 90.39(17), N(1)–Ru(1)–N(2) 173.70(17), Br(1)–Ru(1)–Br(2) 92.80(7), N(1)–Ru(1)–Br(2) 91.47(13), N(2)–Ru(1)–Br(2) 92.68(14), N(1)–Ru(1)–Br(1) 93.24(14), N(2)–Ru(1)–Br(1) 91.29(13).

erage Br−Ru−N(py) angles are 92.42(12)° in **3** and 92.17(3)° in **4**, consistent with the two *cis* terminal bromide atoms.

Each of the cyclic voltammograms of complexes **1** and **2** shows one oxidation peak ($E_{1/2} = 0.82$ V for **1**, $E_{1/2} = -0.42$ V for **2**) and one reduction peak ($E_{1/2} = 0.23$ V for **1**, $E_{1/2} = 0.47$ V for **2**), which are assigned to the Ru^{III}-Ru^{II} couple and ligand-centered oxidation, respectively. It is also noted that each of the cyclic voltammograms of complexes **3** and **4** reveals two reversible couples ($E_{1/2} = -0.59$ V and -1.23 V for **3**, $E_{1/2} = -0.42$ V and -1.27 V for **4**) assigned to the metal-centered oxidation of Ru^{IV}-Ru^{III} and the metal-centered Ru^{III}-Ru^{II} couple, respectively, which are shifted to negative potential compared with that of $Ru(acac)_3$ (oxidation: 0.60 V, reduction: -1.16 V) [24]. All peaks are corresponding to reversible one-electron transfer processes [25]. This may reflect mainly the different redox sites between the reduction and the oxidation in $[Ru(acac)_2(Rpy)_2]/[Ru(acac)(Rpy)_2]^{2+}$ moieties: a ligand acac-based electron transfer takes place in the reduction of Ru-acac-Rpy complexes, while the site of the oxidation is believed to be mainly the central ruthenium atom [26].

In summary, the bis(acetylacetonato)ruthenium(II) complexes *cis*-$[Ru^{II}(acac)_2(Rpy)_2]$ (Rpy = 2-CN-py (**1**), Rpy = 3,5-Me_2-py (**2**)) and the mono(acetylacetonato)ruthenium(III) complexes $[Ru^{III}(acac)Br_2(Rpy)_2]$ (Rpy = 3-Me-py (**3**), Rpy = 3,5-Me_2-py (**4**)) with substituted pyridine ligands were synthesized and structurally characterized including spectroscopic and electrochemical analyses. Formation of complexes **1** and **2** involved the reduction of ruthenium(III) to ruthenium(II) by zinc as reducing agent. Isolation of complexes **3** and **4** involved the displacement of two $acac^-$ ligands in the starting complex by two pyridine molecules and two bromide anions at the $[Ru(acac)]^{2+}$ species. In previous reports on bis(acac)-ruthenium complexes, relatively few mono(acac)-ruthenium complexes such as **3** and **4** have been described. The catalytic properties of these ruthenium-acac-pyridine complexes will be investigated in our laboratory.

Acknowledgement

This project was supported by the Natural Science Foundation of China (20771003 and 21201003). We greatly appreciated helpful suggestions from the reviewers and the editor.

[1] H. Matsuzawa, Y. Ohashi, Y. Kaizu, H. Kobayashi, *Inorg. Chem.* **1988**, *27*, 2981.
[2] P. A. Reynolds, J. W. Cable, A. N. Sobolev, B. N. Figgis, *J. Chem. Soc., Dalton Trans.* **1998**, 559.
[3] S. Patra, B. Mondal, B. Sarkar, M. Niemeyer, G. K. Lahiri, *Inorg. Chem.* **2003**, *42*, 1322.
[4] M. A. Bennett, G. Chung, D. C. R. Hockless, H. Neumann, A. C. Willis, *J. Chem. Soc., Dalton Trans.* **1999**, 3451.
[5] R. D. Ernst, E. Meléndez, L. Stahl, M. L. Ziegler, *Organometallics* **1991**, *10*, 3635.
[6] E. Meléndez, R. Ilarraza, G. P. A. Yap, A. L. Rheingold, *J. Organomet. Chem.* **1996**, *522*, 1.
[7] T. Kobayashi, Y. Nishina, K. G. Shimizu, G. P. Satô, *Chem. Lett.* **1988**, 1137.
[8] T. Manimaran, T.-C. Wu, W. D. Klobucar, C. H. Kolich, G. P. Stahly, *Organometallics* **1993**, *12*, 1467.
[9] A. S. Chan, S. A. Laneman, C. X. Day, *Inorg. Chim. Acta* **1995**, *228*, 159.
[10] B. Sarkar, S. Patra, J. Fiedler, R. B. Sunoj, D. Janardanan, S. M. Mobin, M. Niemeyer, G. K. Lahiri, W. Kaim, *Angew. Chem. Int. Ed.* **2005**, *44*, 5655.
[11] S. Kar, N. Chanda, S. M. Mobin, F. A. Urbanos, M. Niemeyer, V. G. Puranik, R. Jimenez-Aparicio, G. K. Lahiri, *Inorg. Chem.* **2005**, *44*, 1571.
[12] S. Chellamma, M. Lieberman, *Inorg. Chem.* **2001**, *4*, 3177.
[13] S. Patra, B. Sarkar, S. M. Mobin, W. Kaim, G. K. Lahiri, *Inorg. Chem.* **2003**, *42*, 6469.
[14] T. Hashimoto, S. Hara, Y. Shiraishi, K. Natarajan, K. Shimizu, *Chem. Lett.* **2003**, *32*, 874.
[15] J. Shono, Y. Nimura, T. Hashimoto, K. Shimizu, *Chem. Lett.* **2004**, *33*, 1422.
[16] H. Remita, M. E. Brik, J. C. Daran, M. O. Delcourt, *J. Organomet. Chem.* **1995**, *486*, 283.
[17] A. Johnson, G. W. Everett, *J. Am. Chem. Soc.* **1972**, *94*, 1419.
[18] SMART and SAINT+ for Windows NT (version 6.02a), Area Detector Control and Integration Software, Bruker Analytical X-ray Instruments Inc., Madison, Wisconsin (USA) **1998**.

[19] G. M. Sheldrick, SADABS, Program for Empirical Absorption Correction of Area Detector Data, University of Göttingen, Göttingen (Germany) **1996**.
[20] G. M. Sheldrick, SHELXTL (version 5.1), Software Reference Manual, Bruker Analytical X-ray Instruments Inc., Madison, Wisconsin (USA) **1997**.
[21] A. Thorn, G. M. Sheldrick, *Acta Crystallogr.* **2008**, *A64*, C221.
[22] H. Masui, A. B. P. Lever, *Inorg. Chem.* **1993**, *32*, 2199.
[23] H. A. Mirza, A. A. Farah, D. V. Stynes, A. B. P. Lever, *Acta Crystallogr.* **2003**, *E59*, m679.
[24] Y. Kasahara, Y. Hoshino, K. Shimizu, G. P. Satô, *Chem. Lett.* **1990**, 381.
[25] P. Doppelt, T. J. Meyer, *Inorg. Chem.* **1987**, *26*, 2027.
[26] V. T. Coombe, G. A. Heath, T. A. Stephenson, D. A. Tocher, *J. Chem. Soc., Chem. Commun.* **1983**, 303.